Received: 11 January 2022 | Accepted: 28 March 2022

DOI: 10.1002/iub.2616

RESEARCH COMMUNICATION

IUBMB LIFE WILEY

Herbal inhibitors of SARS-CoV-2 M^{pro} effectively ameliorate acute lung injury in mice

Xinyi Du[1] | Longxin Xu[1] | Yiming Ma[1] | Shuaiyao Lu[2] | Kegong Tang[1] | Xiangyu Qiao[1] | Jiaqi Liu[1] | Xiaona Wang[1] | Xiaozhong Peng[1,2] | Chengyu Jiang[1]

[1]State Key Laboratory of Medical Molecular Biology, Institute of Basic Medical Sciences Chinese Academy of Medical Sciences, Department of Biochemistry, School of Basic Medicine Peking Union Medical College, Beijing, China

[2]National Kunming High-level Biosafety Primate Research Center, Institute of Medical Biology, Chinese Academy of Medical Sciences and Peking Union Medical College, Yunnan, China

Correspondence
Chengyu Jiang and Xiaozhong Peng, State Key Laboratory of Medical Molecular Biology, Institute of Basic Medical Sciences Chinese Academy of Medical Sciences, Department of Biochemistry, School of Basic Medicine Peking Union Medical College, Beijing, China.
Email: jiang@pumc.edu.cn (C. J.); pengxiaozhong@pumc.edu.cn (X. P.)

Funding information
Chinese Academy of Medical Sciences Innovation Fund for Medical Sciences, Grant/Award Number: 2021-I2M-1-022; Overseas Expertise Introduction Center for Discipline Innovation ("111 Center"), Grant/Award Number: BP0820029; National Natural Science Foundation of China, Grant/Award Number: 81788101

Abstract

Coronavirus disease 2019, a newly emerging serious infectious disease, has spread worldwide. To date, effective drugs against the disease are limited. Traditional Chinese medicine was commonly used in treating COVID-19 patients in China. Here we tried to identify herbal effective lipid compounds from the lipid library of 92 heat-clearing and detoxication Chinese herbs. Through virtual screening, enzymatic activity and inhibition assays, and surface plasmon resonance tests, we identified lipid compounds targeting the main protease (M^{pro}) of severe acute respiratory syndrome coronavirus 2 (SARS-CoV-2) and verified their functions. Here, we found that natural lipid compounds LPC (14:0/0:0) and LPC (16:0/0:0) could target SARS-CoV-2 M^{pro}, recover cell death induced by SARS-CoV-2, and ameliorate acute lung injury (ALI)/acute respiratory distress syndrome (ARDS) induced by bacterial lipopolysaccharides and virus poly (I:C) mimics in vivo and in vitro. Our results suggest that LPC (14:0/0:0) and LPC (16:0/0:0) might be potential pan remedy against ARDS.

KEYWORDS

ALI/ARDS, M^{pro}, pan-anti-inflammatory, SARS-CoV-2, traditional Chinese medicine

Abbreviations: ALI, acute lung injury; ARDS, acute respiratory distress syndrome; BALF, bronchoalveolar lavage fluid; COVID-19, the novel coronavirus disease 2019; IL-1β, interleukin 1 beta; IL-6, interleukin 6; LPS, bacterial lipopolysaccharide; LTA, lipoteichoic acid; M^{pro}, the main protease; SARS-CoV-2, severe acute respiratory syndrome coronavirus 2; TCM, traditional Chinese medicine; TNF-α, tumor necrosis factor-α.

Xinyi Du, Longxin Xu, and Yiming Ma contributed equally to this work.

1 | INTRODUCTION

Currently, the novel coronavirus disease 2019 (COVID-19) is sweeping worldwide, causing serious public health problems.[1,2] The initial clinical symptom is pneumonia, which usually occurs in the first 3 weeks of symptomatic infection. Significant signs of viral pneumonia include decreased oxygen saturation, abnormal blood gas levels, and visible increases and significant changes in chest radiographs and other imaging techniques.[3] The development of acute respiratory distress syndrome (ARDS) in the middle and later stages of COVID-19 is the most relevant factor for a fatality rate of around 1%–3% due to uncontrollable immune activation, which is called "cytokine storm." It is reported that patients benefit from antiviral drugs in early disease stages and from anti-inflammatory drugs in severe and late-stage disease.[4] COVID-19 pneumonia seriously endangers human life. Veklury (remdesivir) is the only antiviral drug approved by the Food and Drug Administration (FDA) for adults and certain pediatric patients with COVID-19, and the FDA has issued an emergency use authorization for Paxlovid, Molnupiravir, and several monoclonal antibody treatments for COVID-19. Until now, there is no specific drug that can both target the SARS-CoV-2 to block viral replication and simultaneously alleviate symptoms and reduce patients' cytokine storm. We propose a novel drug therapy strategy that could target the virus while reducing patients' cytokine storm, making it possible to be used for the whole course in patients with COVID-19.

SARS-CoV-2 is an enveloped, positive, single-stranded RNA virus that is highly infectious.[5] SARS-CoV-2 genome annotation revealed 14 open reading frames (ORFs), including orf1ab, orf1a, four main structural genes, and eight accessory genes. Two cysteine proteases are encoded by orf1a, a 3C-like protease ($3CL^{pro}$), and a papain-like protease (PL^{pro}). $3CL^{pro}$ is also known as the main protease (M^{pro}), an indispensable enzyme in the process of virus replication and infection.[6,7] M^{pro} is highly conserved in coronavirus and shares no homology with counterparts in human beings. Therefore, drug development for M^{pro} can substantially reduce mutation-mediated drug resistance, which makes M^{pro} an ideal target for antiviral therapy.[8] M^{pro} inhibitors hold great promise.

Traditional Chinese medicine (TCM) has a long history and plays an indispensable role in the prevention and treatment of various epidemics. TCM decoctions comprise chemical compounds, lipids, proteins, and sRNAs,[9] and lipid compounds have been found to play essential roles in virus infection, inflammation, and other diseases.[10–14]

Accordingly, we selected the relevant herbs, extracted and identified the main lipid components, established an in-house natural lipid database to screen M^{pro} inhibitors, and explored its broad-spectrum anti-inflammatory effects.

2 | MATERIALS AND METHODS

2.1 | Reagents

LPC (14:0/0:0) (CAS number: 20559–16-4, #855575P), LPC (16:0/0:0) (CAS number: 17364–16-8, #855675P), PC (9:0/9:0) (CAS number: 27869–45-0, #850320P), and PC (16:0/18:1) (CAS number: 26853–31-6, #850457P) were purchased from Sigma-Aldrich, Inc. (St. Louis, MO) and DG (16:0/18:0) (CAS number: 17708–08-06, #32–1,654) was purchased from Larodan Inc. (Sweden). The fluorescently labeled substrate of SARS-CoV-2 M^{pro}, MCA-AVLQ SGFR-Lys (Dnp)-Lys-NH_2, was purchased from GL Biochemistry Ltd. Recombinant SARS-CoV-2 M^{pro} ($3CL^{pro}$) was purchased from MedChemExpress (Monmouth Junction, NJ). Roswell Park Memorial Institute 1,640 (RPMI-1640), Ham's F-12 nutrient mixture (F-12), minimal essential organ culture medium (MEM), and fetal bovine serum (FBS) were obtained from Gibco BRL (Grand Island, NY). (3-(4,5-dimethylthiazol-2-yl)-5-(3-carboxymethoxyphenyl)-2-(4-sulfophenyl)-2H (MTS) was purchased from Promega (Promega Corporation, WI). Bacterial lipopolysaccharide (LPS) from Escherichia coli 0111:B4 (#L4391), synthetic double-stranded RNA poly (I:C) (#P1530), and lipoteichoic acid (LTA) from *Enterococcus hirae* (#L4015) were purchased from Sigma-Aldrich, Inc. (St. Louis, MO).

2.2 | Establishment of a natural in-house lipid database

Ninety-two herbs were purchased from Beijing Tong Ren Tang Co. Ltd. (China). The preparation of lipid samples of herb decoctions was described previously.[9,15] HPLC-MS/MS was used for untargeted analysis of extracted lipid samples. Sample analysis was performed using an ExionLC (SCIEX, USA) coupled with a TripleTOF 5,600+ (SCIEX, USA) in both positive and negative ionization modes. The original data were imported into Progenesis QI (Waters) for data preprocessing, alignment, deconvolution, peak extraction, and metabolite identification. After the data were imported, QC samples were selected as references for peak alignment, and the linear weighted moving average method was used to smooth the peaks. The smoothing level was two scans, and each peak was composed of at least five scans. LIPID MAPS® was used to identify the compounds. Then we selected lipid

compounds with relative intensity values greater than 50,000 to construct a database of major lipid compounds in the herbs' decoctions, with a total of 1,407 molecules.

2.3 | Docking-based virtual screening

Discovery Studio 2020 was used to conduct virtual screening. "Prepare Ligands" and "Full minimization" modules were used to prepare lipid compounds. All structures were filtered according to Lipinski's rule of five and refined again with the "toxicity prediction" tool to filter out potential carcinogenic, mutagenic, and teratogenic compounds. Through the above screening conditions, we obtained the drug-like set.

The M^{pro} structure (PDB code 6LU7) was downloaded from the Protein Data Bank (www.rcsb.org). LibDock and CDOCKER programs were used for docking among drug-like set. M^{pro}-N3 was employed as the template, and the other docking parameters were set to default values in the two docking programs.

2.4 | Enzymatic activity and inhibition assays

The enzyme activity and inhibition assays were performed using conventional methods, as previously described.[16] The recombinant SARS-CoV-2 M^{pro} (30 nM final concentration) was mixed with serial dilutions of the lipid compound dissolved in 100% DMSO in 80 μl assay buffer (50 nM Tris–HCl, pH 7.3, 1 mM EDTA) and incubated for 30 min. An equal volume of DMSO without any compound was used as the negative control. The reaction was initiated by adding 40 μl of a fluorogenic substrate (20 μM final concentration). The fluorescence signal at 320 nm (excitation)/405 nm (emission) was immediately measured every 30 s for 10 min using a plate reader (Varioskan™ LUX, Thermo Scientific™). The IC_{50} values against SARS-CoV-2 M^{pro} were measured at 10 lipid compound concentrations, and three sets of wells were used for each concentration experiment. The V_{max} values of reactions involving the lipid compounds added at various concentrations and the negative control were obtained by fitting the Michaelis–Menten equation. The inhibition rate was calculated based on V_{max} and was used to generate the IC_{50} curves.

2.5 | Surface plasmon resonance (SPR) detection

SPR experiments were performed using a Biacore T200 (GE Healthcare) at 25°C. Amine coupling chemistry was used to immobilize the SARS-CoV-2 M^{pro} protein on a carboxymethyl-5′-dextran (CM5) sensor chip, M^{pro} was fixed in four channel flow cells, and three channels were used as reference for activation and closure. The SARS-CoV-2 M^{pro} proteins (22.5 μg·ml^{-1} in 10 mM sodium acetate, pH 4.5) were immobilized on the surface over a 420 second injection period. The remaining activated groups on the surface were blocked with a 420-s injection of 1 M ethanolamine at pH 8.5. For all the above procedures, the flow rate was maintained at 30 μl·min^{-1}, and a 1 × phosphate-buffered saline running buffer was used during immobilization. Approximately 9,000 protein response units could be routinely captured on the CM5 chip on flow cells.

2.6 | Cells and virus

The human acute monocytic leukemia cell line THP-1, human lung adenocarcinoma cell line A549, human histiocyte lymphoma cell line U937, and Vero E6 cell line were purchased from the Peking Union Medical College Cell Culture Center. No mycoplasma contamination was detected in cells. THP-1 cells and U937 cells were grown in RPMI-1640 medium, A549 cells were grown in Ham's F-12 medium, and Vero E6 cells were grown in MEM medium, and all were supplemented with 10% FBS and 1% Pen/Strep under standard conditions. Cells were cultured in a 37°C incubator with 5% CO_2. SARS-CoV-2 infected tests were performed in a biosafety level-3 (BLS-3) laboratory of the National Kunming High-Level Biosafety Primate Research Center (Yunnan, China).

2.7 | Antiviral activities in vitro

Vero E6 cells were plated in a 96-well dish. At 60% confluence, cells were pre-treated with 50 μM lipid compounds respectively, which were dissolved in 100% DMSO. After 24 hr, Vero E6 cells were infected with SARS-CoV-2 (MOI = 0.4). After 48 hr infection, cell images were taken for analysis of cytopathic effect (CPE) and cell viabilities were measured by the MTS assay according to the manufacturer's instructions.

2.8 | LPS-, poly (I:C)- or LTA-induced cell models

In 12-well culture plates, cells were pre-treated with 100 μM of each candidate lipid for 12 hr. The five candidate lipids were dissolved in 100% DMSO. Twelve hours after pretreatment, THP-1 cells, A549 cells, or U937 cells

were infected with 10 μg·ml^{-1} LPS, 1 μg·ml^{-1} poly (I:C), or 10 μg·ml^{-1} LTA, respectively. After 12 hr, supernatants and cells were collected for subsequent experiments.

2.9 | Animals

Six-week-old male Balb/c mice were purchased from Vital River (Beijing, China). All mice were maintained in pathogen-free conditions at Peking Union Medical College under a standard protocol of the Animal Care and Use Committee at the Institute of Basic Medical Sciences, Chinese Academy of Medical Sciences and Peking Union Medical College. Animal care and surgical procedure were performed following the National Institute of Health Guide for the Care and Use of Laboratory Animals.

2.10 | LPS- or poly (I:C)-induced acute lung injury (ALI) mouse models

Mice were orally administered 30 mg·kg^{-1} LPC (16:0/0:0) or LPC (14:0/0:0) for 3 days. LPC (16:0/0:0) and LPC (14:0/0:0) were dissolved in a solvent consisting of 5% DMSO, 10% Kolliphor HS 15, and 85% saline. Twelve hours after gavage on the third day, the Balb/c mice were anesthetized, and 10 mg·kg^{-1} LPS or 25 mg·kg^{-1} poly (I:C) suspended in sterile saline were administered intratracheally to induce ALI. Saline alone was treated for the control animals. The mice were euthanized 12 hr after LPS administration and euthanized 9 hr after poly (I:C) administration ($n = 6$ per group). Bronchoalveolar lavage fluid (BALF), plasma, and lung tissues of mice were collected for further detection.

2.11 | Cytokines detection

Cytokines in the cell supernatants, mouse BALF, and mouse plasma were analyzed using enzyme-linked immunosorbent assay (ELISA) methods for protein expression level. ELISA kits were purchased from R&D Systems. mRNA expression level was detected by quantitative real-time PCR (RT-qPCR). RNA was extracted using the TRIzol reagent (Sigma-Aldrich) and reverse-transcribed using PrimeScript™ RT Master Mix (Takara). RT-qPCR was performed using the LightCycler 480 SYBR Green I Master kit and LightCycler 480 PCR System (Roche, Switzerland). The relative human gene and mouse gene expression levels were calculated using the ΔΔCt method and normalized to the human reference gene *UBC* and the mouse reference gene *Gapdh*, respectively. Detailed sequence information regarding the primers is shown in Table S3.

2.12 | Histopathological and lung injury score

Histopathological examination of lung tissues was performed with hematoxylin–eosin (H&E). The slices were observed using a light microscope (Leica Microsystems, Wetzlar, Germany). Lung injury was scored using a five-point scale in accordance with the combined assessment of alveolar congestion, hemorrhage, infiltration or aggregation of neutrophils in the airspace or vessel wall, and the thickness of alveolar wall/hyaline membrane formation: 0, minimum damage; 1, mild damage; 2, moderate damage; 3, severe damage, and 4, maximum damage.[17]

2.13 | Statistical analysis

Data are expressed as means ± SEM. All experiments were repeated at least thrice. Differences in measured variables in different treatment groups were assessed using Student's *t*-test. Results were considered statistically significant at $p < .05$. GraphPad Prism 8.0 (GraphPad Software, Inc., San Diego, CA) was used for the statistical analysis.

3 | RESULTS

3.1 | Virtual screening based on natural in-house lipid database

Based on the effect of heat-clearing and detoxication, 92 types of herbs (Table S1) were selected to construct our TCM lipid database. We found that most of them were included in the "Diagnosis and Treatment Protocol for COVID-19" and COVID-19 related TCM prescriptions. Via lipidomic analysis, we selected lipid compounds with relative intensity values greater than 50,000 to construct a library of major lipid compounds in the herbs, with a total of 1,407 molecules. The flowchart for establishing a lipid database is shown in Figure S1A. Subsequently, we classified the lipid database according to the LIPID MAPS® Lipid Classification System, and found it covers a wide range of categories (Figure S1B). We finally identified five lipid compounds via virtual screening, which are commercially available

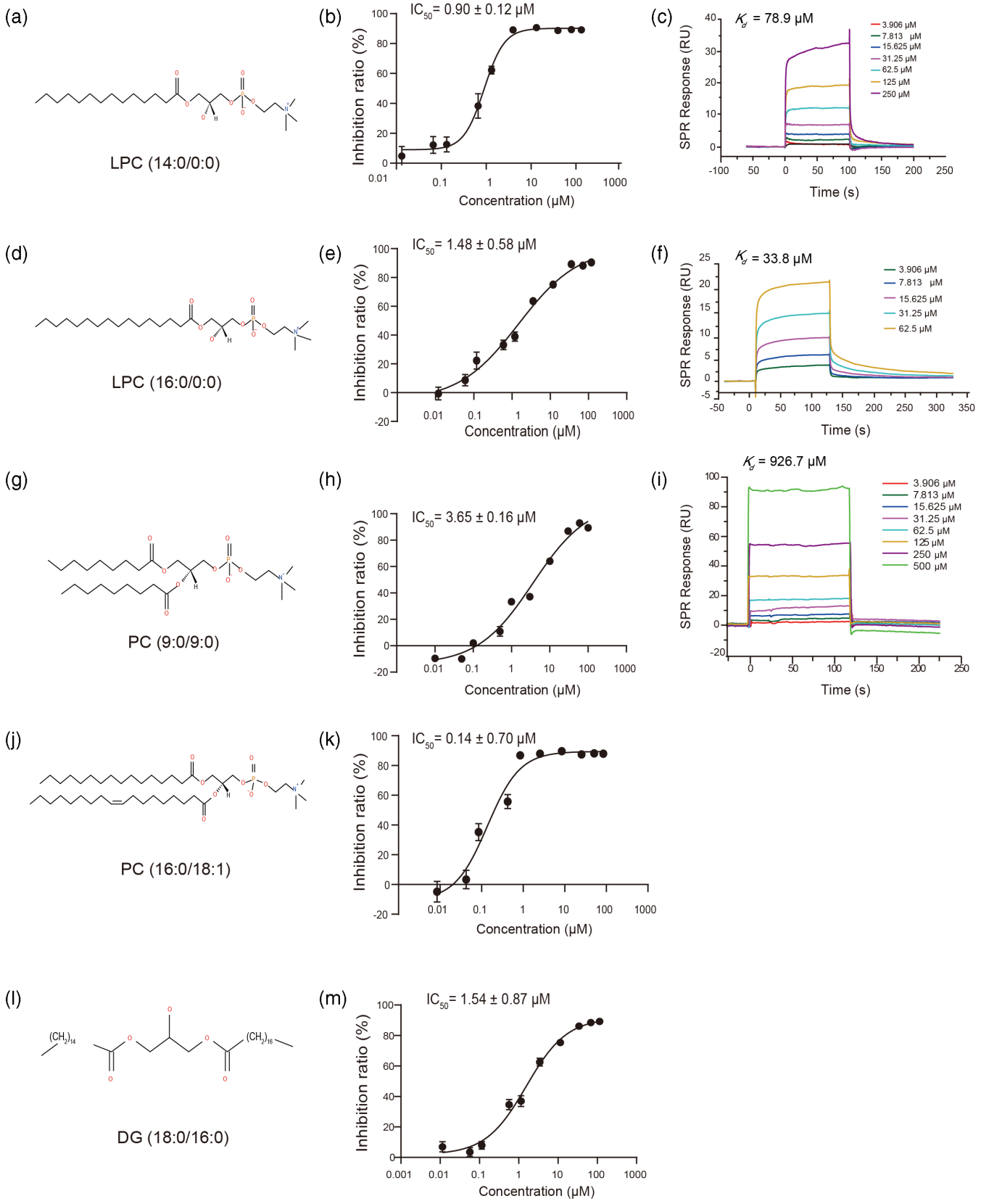

FIGURE 1 Lipid compounds action against SARS-CoV-2 M^{pro}. (a-c) LPC (14:0/0:0). (d-f) LPC (16:0/0:0). (g-i) PC (9:0/9:0). (j and k) PC (16:0/18:1). (l and m) DG (18:0/16:0). The lipid compound structures formulas are shown on the left. The hydrolytic activity of SARS-CoV-2 M^{pro} was measured in the presence of increasing concentrations of lipid candidates. An increasing amount of ligand was titrated to the M^{pro} protein and investigated using SPR and the calculated K_d values

TABLE 1 The binding capacity of five lipid compounds with M^{pro}

Lipid name	Affinity(kcal/Mol)	SPR (μM)	IC_{50} (μM)
LPC (14:0/0:0)	75.2	78.9	0.90 ± 0.12 μM
LPC (16:0/0:0)	80.1	33.8	1.48 ± 0.58 μM
PC (9:0/9:0)	93.3	926.7	3.65 ± 0.16 μM
PC (16:0/18:1)	77.5	\	0.14 ± 0.70 μM
DG (16:0/18:0)	65.7	\	1.54 ± 0.87 μM

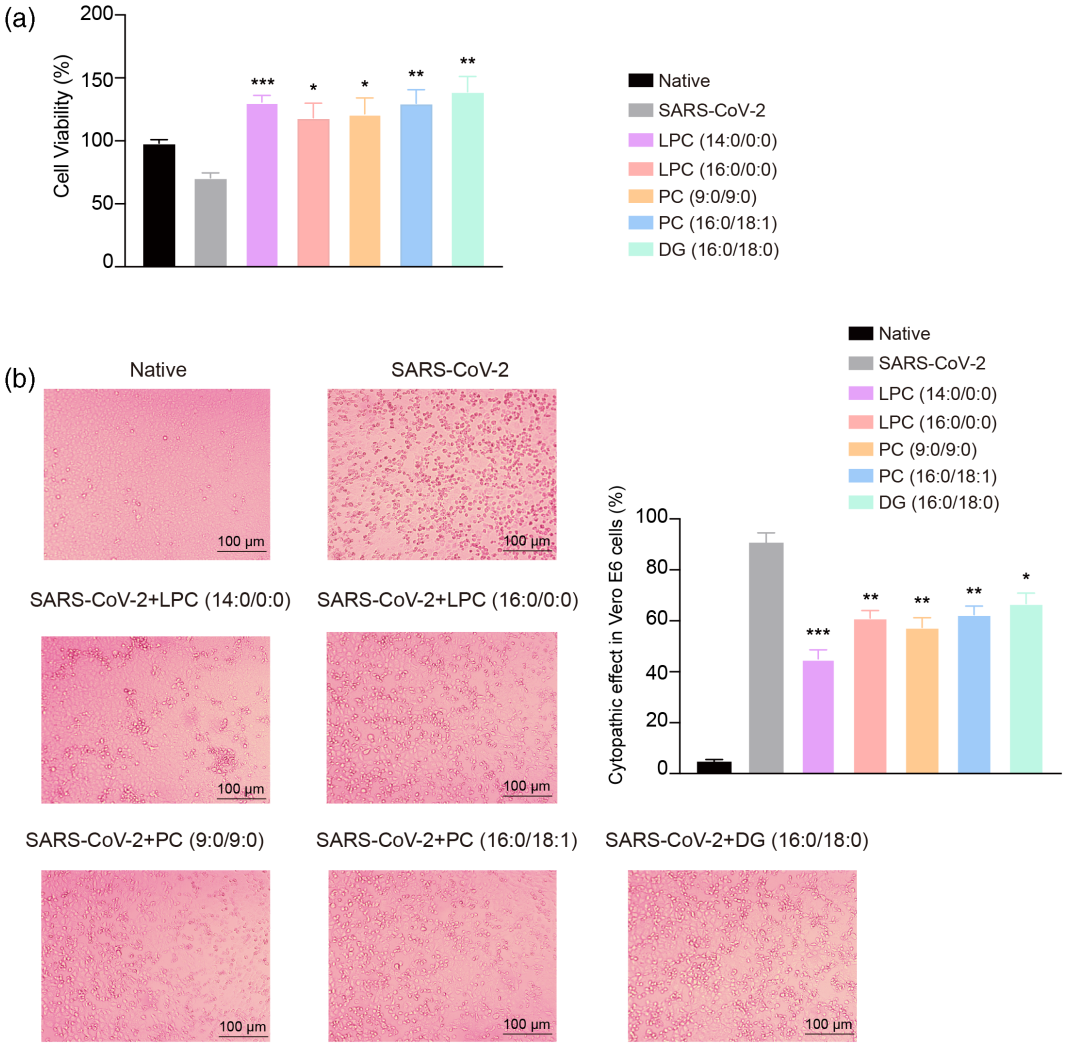

FIGURE 2 Lipid compounds rescued cell death in SARS-CoV-2 infection. (a) Cell viability of SARS-CoV-2-infected Vero E6 cells. Cell viabilities were measured via MTS assay 48 hr after infection. (b) Cytopathic effect of SARS-CoV-2 infected Vero E6 cells treated with five lipid compounds. Vero E6 cells were treated with 50 μM of each lipid candidate. After 24 hr, Vero E6 cells were infected with 0.4 MOI SARS-CoV-2 viral particles. Images under a NiKon Eclipse TE300 microscope (NiKon Corporation, Tokyo, Japan) at 100 magnification. *$p < .05$; **$p < .01$; ***$p < .001$

and inexpensive but with high affinity for SARS-CoV-2 M^{pro}. The molecular docking results are shown in Figure S1C. Four of the lipids are glycerophospholipids, and the lipid compound DG (16:0/18:0) is a glycerolipid. Information on the five lipid compounds is shown in Table S2.

3.2 | Experimental verification of the candidate lipid compounds against M^{pro} in vitro

To verify the docking results, SPR tests, enzymatic activity, and inhibition assays were conducted to confirm

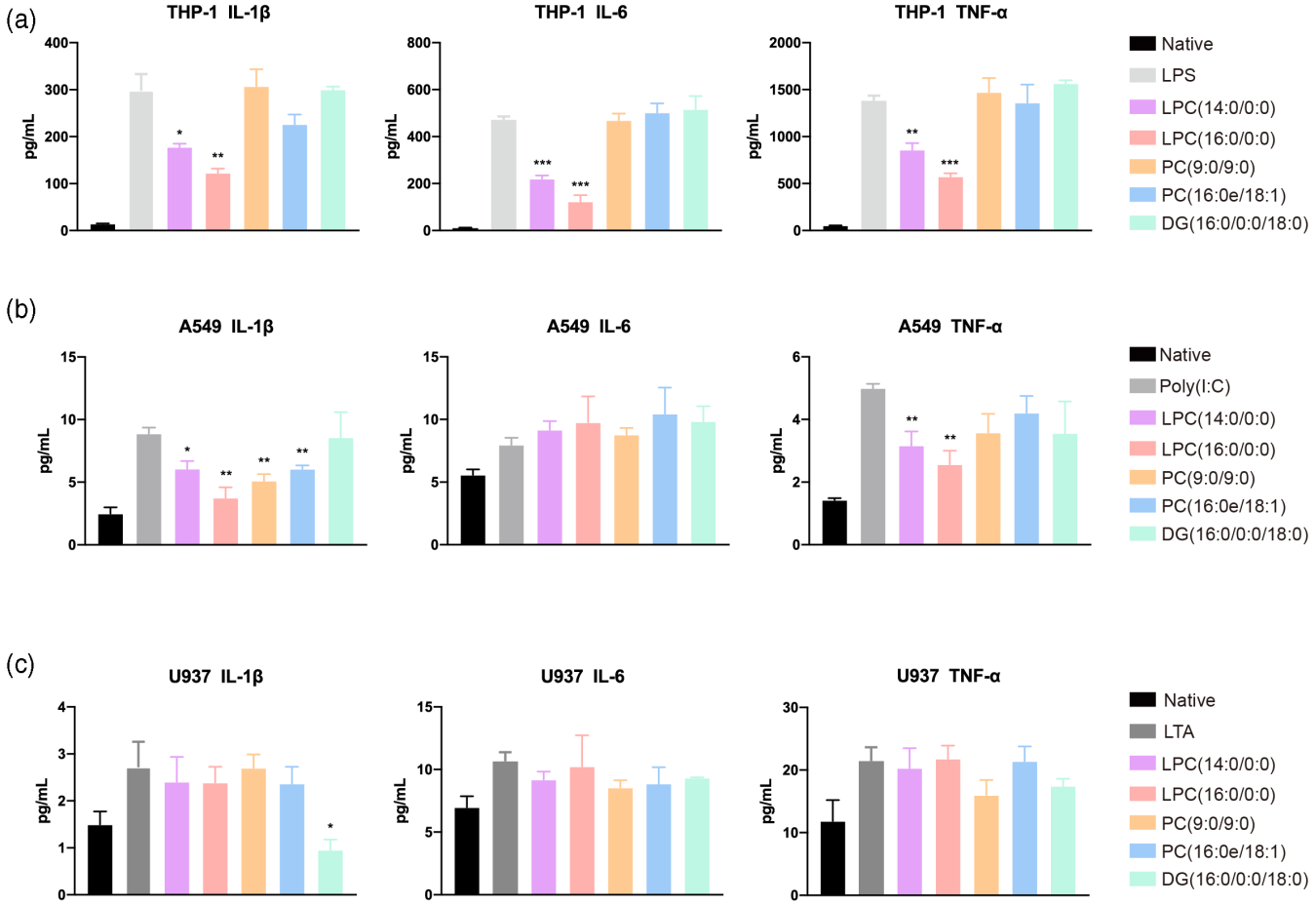

FIGURE 3 Effect of lipid compounds treatment on the protein expression level of inflammatory cytokines in LPS-, poly (I:C)-, and LTA-induced cell models. (a) ELISA analysis of cytokine (IL-1β, IL-6, and TNF-α) expression levels in the supernatants of THP-1 cells induced by LPS. (b) ELISA analysis of cytokine (IL-1β, IL-6, and TNF-α) expression level in the supernatants of A549 cells induced by poly (I:C). (c) ELISA analysis of cytokine (IL-1β, IL-6, and TNF-α) expression level in the supernatants of U937 cells induced by LTA. In 12-well culture plates, cells were treated with 100 μM of each lipid candidate for 12 hr, and THP-1 cells, A549 cells, or U937 cells were infected with 10 $\mu g \cdot ml^{-1}$ LPS, 1 $\mu g \cdot ml^{-1}$ poly (I:C), or 10 $\mu g \cdot ml^{-1}$ LTA, respectively. After 12 hr, supernatants were collected, and inflammatory factor levels were detected using ELISA. *$p < .05$; **$p < .01$; ***$p < .001$

candidate compounds that could bind to SARS-CoV-2 M^{pro} and inhibit its hydrolytic activity in vitro. As illustrated in Figure 1a–m, LPC (14:0/0:0) showed binding affinity with a K_d value of 78.9 μM and inhibitory potency with an IC_{50} value of 0.92 ± 0.12 μM. LPC (16:0/0:0) showed binding affinity with a K_d value of 33.8 μM and inhibitory potency with an IC_{50} value of 1.48 ± 0.58 μM, whereas PC (9:0/9:0) showed binding affinity with a K_d value of 926.7 μM and inhibitory potency with an IC_{50} value of 3.65 ± 0.16 μM. PC (16:0/18:1) and DG (16:0/18:0) obtained no SPR test results due to poor solubility, and their inhibitory potencies showed IC_{50} values of 0.14 ± 0.70 μM and 1.54 ± 0.87 μM, respectively (Table 1). We verified the combined capacity of the candidate lipid compounds with M^{pro} from multiple perspectives and proved that they are effective inhibitors of M^{pro} in vitro.

3.3 | The candidate lipid compounds potently inhibit SARS-CoV-2 in Vero E6 cells

The previous results confirmed that the five lipid compounds could inhibit the M^{pro} of SARS-CoV-2 by direct binding, and we detected the antiviral effect at the cellular level. The five lipid compounds could significantly improve cell viability at the concentration of 50 μM, which was assayed in Vero E6 cell line induced by SARS-CoV-2 (Figure 2a). In CPE inhibition assay, SARS-CoV-2-induced Vero E6 cells exhibited severe CPE, including cell rounding, detachment, and death. SARS-CoV-2-induced CPE was markedly ameliorated after 48 hr incubation at the same concentration of the five lipid compounds (Figure 2b).

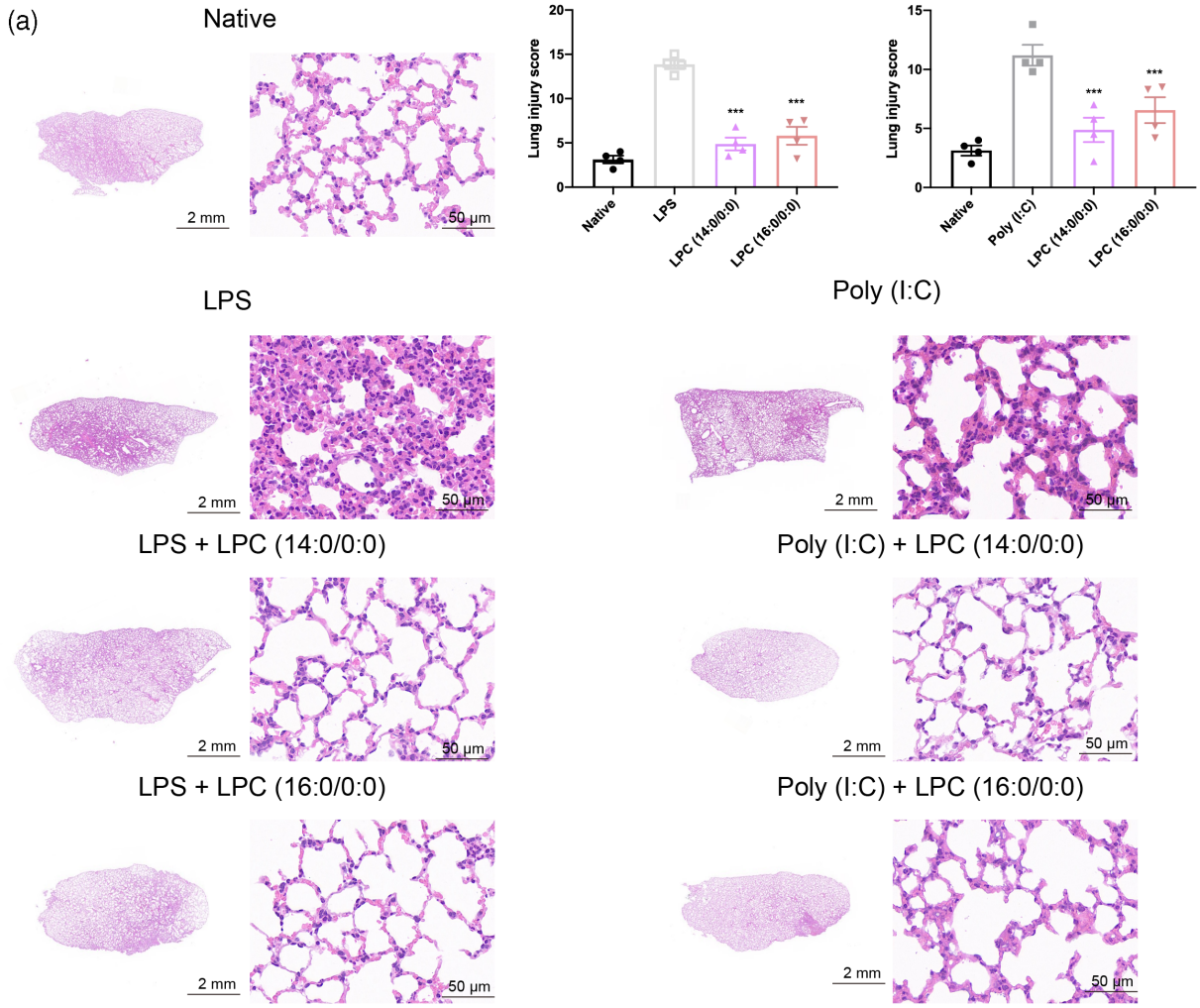

FIGURE 4 LPC (14:0/0:0) and LPC (16:0/0:0) pretreatment ameliorate LPS- and poly (I:C)-induced ALI in mice. (a) H&E staining and lung injury score of mouse lung tissues infected by LPS or poly (I:C). Balb/c mice were gavaged with 30 mg·kg^{-1} LPC (14:0/0:0) or LPC (16:0/0:0) for 3 days and intratracheally injected with 10 mg·kg^{-1} LPS or 25 mg·kg^{-1} poly (I:C). ($n = 4$ each group). ***$p < .001$

3.4 | Anti-inflammatory effect of the candidate lipid compounds in cells treated with virus poly (I:C) mimics, bacterial components LPS and LTA

ARDS is one of the main causes of SARS-CoV-2-related deaths. Because of the significant anti-SARS-CoV-2 effect of the candidate lipid compounds, we performed cell assays of the gram-negative bacteria component LPS, gram-positive bacteria component LTA, and virus poly (I:C) mimics to further evaluate their anti-inflammatory effects. Our data showed that two lipid compounds could reduce the LPS- and poly (I:C)-induced pro-inflammatory cytokines at both the protein and mRNA levels (Figure 3a,b, Figure S2A,B). However, in the LTA-induced U937 cell model, the effect was not obvious (Figure 3c and Figure S2C). Furthermore, LPC (14:0/0:0) and LPC (16:0/0:0) can reduce pro-inflammatory cytokines induced by LPS and poly (I:C) in a dose-dependent manner (Figure S3A–D). Based on the previous results, we selected LPC (14:0/0:0) and LPC (16:0/0:0) for further study to identify their pan-anti-ALI effects in vivo.

3.5 | LPC (14:0/0:0) and LPC (16:0/0:0) pretreatment ameliorate lung damage in LPS- and poly (I:C)-induced ALI/ARDS

The pharmacological effects of LPC (14:0/0:0) and LPC (16:0/0:0) were verified in an ALI mouse model induced by LPS and poly (I:C). As detected by H&E staining (Figure 4), LPC (14:0/0:0) and LPC (16:0/0:0) pre-treatment alleviated pulmonary edema and neutrophil

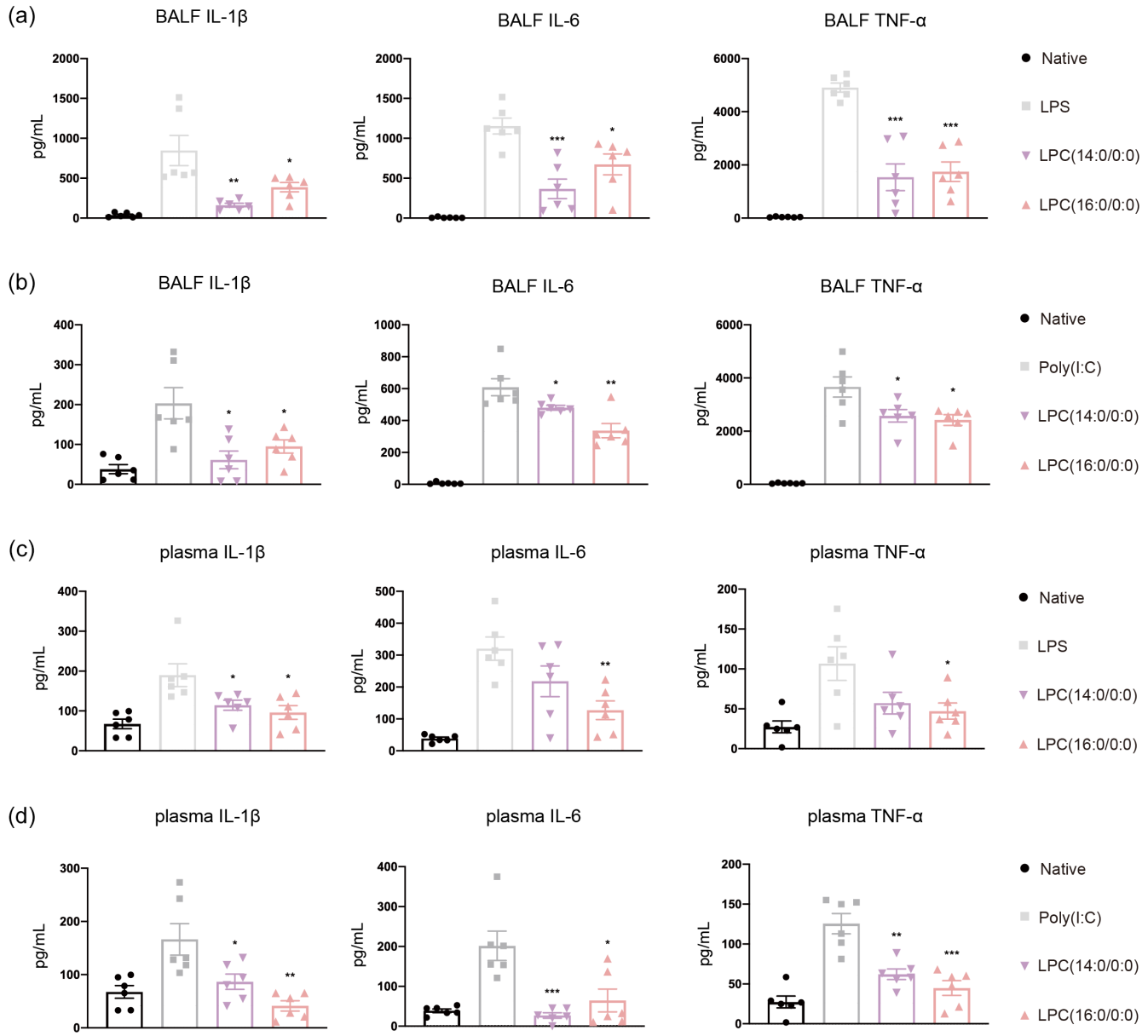

FIGURE 5 LPC (14:0/0:0) and LPC (16:0/0:0) pretreatment reduced cytokine level in the BALF and plasma of ALI model mice induced by LPS or poly (I:C). (a) The BALF cytokine (IL-1β, IL-6, and TNF-α) levels in the LPS-induced mouse model were measured through ELISA. (b) The BALF cytokine (IL-1β, IL-6, and TNF-α) levels in the poly (I:C)-induced mouse model were measured through ELISA. (c) The plasma cytokine (IL-1β, IL-6, and TNF-α) levels in the LPS-induced mouse model were measured through ELISA. (d) The plasma cytokine (IL-1β, IL-6, and TNF-α) levels in the poly (I:C)-induced mouse model were measured through ELISA. Balb/c mice were gavaged with 30 mg·kg^{-1} LPC (14:0/0:0) or LPC (16:0/0:0) for 3 days and intratracheally injected with 10 mg·kg^{-1} LPS or 25 mg·kg^{-1} poly (I:C). ($n = 6$ for each group). The indicators were detected 12 hr after induction with LPS or poly (I:C). *$p < .05$; **$p < .01$; ***$p < .001$

infiltration and showed lower lung injury scores. To evaluate lung inflammation, we measured the levels of pro-inflammatory cytokines, including IL-1β, IL-6, and TNF-α, in BALF and plasma at both the protein and mRNA levels (Figure 5a–d, Figures S4A–D and S5A–D). LPC (14:0/0:0) and LPC (16:0/0:0) also have effective therapeutic effects in LPS- and poly (I:C)-induced mice models, indicating that our lipid compounds might act as pan-anti-ARDS candidate drugs.

4 | DISCUSSION

In the past two decades, new sources of viral infection have emerged, causing epidemics, such as SARS and Middle East respiratory syndrome.[18] The timely development of effective antiviral drugs for clinical use is challenging. Therefore, we used highly conserved M^{pro} as a drug target for virtual screening of major lipid compounds derived from 92 herbs. Based on TCM and

computer-aided drug screening technology, we rapidly identified candidate compounds to conduct anti-COVID-19 and anti-inflammatory research.

We chose lipid compounds to build the screening library because lipid compounds have been neglected as effective TCM components. However, lipids and lipid-like molecules account for up to 7% of all drugs listed on DrugBank (www.drugbank.com). The pharmacological effects of lipid compounds derived from TCM should be paid attention to. Meanwhile, M^{pro} inhibitors have broad-spectrum activity against coronaviruses, including SARS-CoV and MERS-CoV.[19] M^{pro} is an attractive drug target with broad prospects. According to DrugBank, there are 66 experimental unapproved treatments for COVID-19, four of which are M^{pro} inhibitors. Currently, Pfizer has unveiled the first oral M^{pro} inhibitor drug, Paxlovid. The results of Phase III clinical trials showed Paxlovid could reduce the risk of hospitalization or death in mild and moderate adults by 89% compared with placebo.

Previous studies have shown that the main cause of SARS-CoV-2-related deaths is ARDS due to a cytokine storm and dysfunctional immune responses.[20–22] Our study found that natural candidate compounds LPC (14:0/0:0) and LPC (16:0/0:0) were potent inhibitors of SARS-CoV-2 M^{pro} and could effectively inhibit its hydrolytic activity and reduce SARS-CoV-2-induced cytopathic effects. While suppressing the virus, candidate compounds could ameliorate lung injury and reduce high pro-inflammatory cytokines levels caused by the bacterial component LPS and virus poly (I:C) mimics in vivo and in vitro. The screened candidate compounds showed both viral load reduction and anti-inflammatory properties, which might be promising for the treatment of COVID-19. However, due to the limited experimental conditions, we have not verified the results using SARS-CoV-2-infected animals yet, and we plan to carry out such research in the future.

So far, there are no strong clinical evidence supporting the efficacy of any other drugs against SARS-CoV-2, except for intravenous remdesivir and dexamethasone, which have modest effects in moderate to severe COVID-19.[4] Remdesivir has limited use accounting for its administration and indications, and dexamethasone, as a kind of glucocorticoids drug, may modulate inflammation-mediated lung injury and thereby slow down the progression of respiratory failure and death. However, studies have shown that dexamethasone can reduce the mortality of severe patients, but premature medication may be a potential risk.[23] The onset of COVID-19 has a certain incubation period,[24] so it is important to choose the appropriate treatment at the right time. Candidate compounds LPC (14:0/0:0) and LPC (16:0/0:0) developed through our drug screening strategy can target virus while reducing cytokine storms in patients, potentially upending existing therapies. In addition, the candidate compounds were mainly found in Chi Xiao Dou (Vignae Semen), Chuan Xiong (Chuanxiong Rhizoma), and Ren Shen (Ginseng Radix Et Rhizoma), suggesting that they can be used more widely in COVID-19 patients.

ACKNOWLEDGEMENTS

This work is supported by the National Natural Science Foundation of China (81788101), the Chinese Academy of Medical Sciences Innovation Fund for Medical Sciences (2021-I2M-1-022), and the Overseas Expertise Introduction Center for Discipline Innovation ("111 Center") (BP0820029).

CONFLICT OF INTEREST

The authors declare that they have no conflict of interest.

AUTHOR CONTRIBUTIONS

Chengyu Jiang conceived the project and guided the study. Chengyu Jiang, Xiaozhong Peng, Xinyi Du, Longxin Xu, and Yiming Ma designed the study and analyzed the data. Yiming Ma and Xinyi Du performed the virtual screening and validation of M^{pro}. Shuaiyao Lu and Kegong Tang conducted the anti-SARS-CoV-2 test in vitro. Xinyi Du and Longxin Xu conducted the experiments on the ARDS/ALI models in vivo and in vitro. Xiangyu Qiao helped with lipidomics data analysis. Jiaqi Liu and Xiaona Wang helped with the experiments on mice. Chengyu Jiang, Xinyi Du, Longxin Xu, and Yiming Ma wrote the manuscript, and all authors commented and approved the manuscript.

ORCID

Chengyu Jiang https://orcid.org/0000-0003-0570-2709

REFERENCES

1. Velavan TP, Meyer CG. The COVID-19 epidemic. Tropical Med Int Health. 2020;25:278–280.
2. Wang C, Horby PW, Hayden FG, Gao GF. A novel coronavirus outbreak of global health concern. Lancet. 2020;395:470–473.
3. Zhao N, Shi J, Zeng L, Yang S. Clinical characteristics and coping strategies of neoplasms with 2019 novel coronavirus infection. Zhongguo Fei Ai Za Zhi. 2020;23:261–266.
4. Asselah T, Durantel D, Pasmant E, Lau G, Schinazi RF. COVID-19: Discovery, diagnostics and drug development. J Hepatol. 2021;74:168–184.
5. Krammer F. SARS-CoV-2 vaccines in development. Nature. 2020;586:516–527.
6. Wu A, Peng Y, Huang B, et al. Genome composition and divergence of the novel coronavirus (2019-nCoV) originating in China. Cell Host Microbe. 2020;27:325–328.

7. Jo S, Kim S, Shin DH, Kim MS. Inhibition of SARS-CoV 3CL protease by flavonoids. J Enzyme Inhib Med Chem. 2020;35:145–151.
8. Jin Z, Wang H, Duan Y, Yang H. The main protease and RNA-dependent RNA polymerase are two prime targets for SARS-CoV-2. Biochem Biophys Res Commun. 2021;538:63–71.
9. Li X, Liang Z, Du J, et al. Herbal decoctosome is a novel form of medicine. Sci China Life Sci. 2019;62:333–348.
10. Gu S, Li L, Huang H, Wang B, Zhang T. Antitumor, antiviral, and anti-inflammatory efficacy of essential oils from Atractylodes macrocephala Koidz. Produced with Different Processing Methods Molecules. 2019;24.
11. Silva J, Figueiredo PLB, Byler KG, et al. Essential oils as antiviral agents. Potential of essential oils to treat SARS-CoV-2 infection: An in-silico investigation. Int J Mol Sci. 2020;21:10.
12. Armugam A, Cher CD, Lim K, et al. A secretory phospholipase A2-mediated neuroprotection and anti-apoptosis. BMC Neurosci. 2009;10:120.
13. Aoki M, Aoki H, Ramanathan R, et al. Sphingosine-1-phosphate signaling in immune cells and inflammation: Roles and therapeutic potential. Mediat Inflamm. 2016;2016:8606878.
14. Ma Y, Du X, Zhao D, et al. 18:0 Lyso PC, a natural product with potential PPAR-gamma agonistic activity, plays hypoglycemic effect with lower liver toxicity and cardiotoxicity in db/db mice. Biochem Biophys Res Commun. 2021;579:168–174.
15. Bligh EG, Dyer WJ. A rapid method of total lipid extraction and purification. Can J Biochem Physiol. 1959;37:911–917.
16. Yang H, Xie W, Xue X, et al. Design of wide-spectrum inhibitors targeting coronavirus main proteases. PLoS Biol. 2005;3:e324.
17. Wang L, Huang X, Kong G, et al. Ulinastatin attenuates pulmonary endothelial glycocalyx damage and inhibits endothelial heparanase activity in LPS-induced ARDS. Biochem Biophys Res Commun. 2016;478:669–675.
18. de Wit E, van Doremalen N, Falzarano D, Munster VJ. SARS and MERS: Recent insights into emerging coronaviruses. Nat Rev Microbiol. 2016;14:523–534.
19. Zhang L, Lin D, Sun X, et al. Crystal structure of SARS-CoV-2 main protease provides a basis for design of improved alpha-ketoamide inhibitors. Science. 2020;368:409–412.
20. Guan WJ, Ni ZY, Hu Y, et al. Clinical characteristics of coronavirus disease 2019 in China. N Engl J Med. 2020;382:1708–1720.
21. Mehta P, McAuley DF, Brown M, et al. COVID-19: Consider cytokine storm syndromes and immunosuppression. Lancet. 2020;395:1033–1034.
22. Zhang H, Zhou P, Wei Y, et al. Histopathologic changes and SARS-CoV-2 immunostaining in the lung of a patient with COVID-19. Ann Intern Med. 2020;172:629–632.
23. Group RC, Horby P, Lim WS, et al. Dexamethasone in hospitalized patients with Covid-19. N Engl J Med. 2021;384:693–704.
24. Lauer SA, Grantz KH, Bi Q, et al. The incubation period of coronavirus disease 2019 (COVID-19) from publicly reported confirmed cases: Estimation and application. Ann Intern Med. 2020;172:577–582.

SUPPORTING INFORMATION

Additional supporting information may be found in the online version of the article at the publisher's website.

How to cite this article: Du X, Xu L, Ma Y, Lu S, Tang K, Qiao X, et al. Herbal inhibitors of SARS-CoV-2 M^{pro} effectively ameliorate acute lung injury in mice. IUBMB Life. 2022;74(6):532–42. https://doi.org/10.1002/iub.2616